

Mechanistic Studies of Carbon Dioxide Insertion into Metal Hydrides and Extrusion from the Corresponding Metal Formates Utilizing Group 6 Metal Carbonyl Derivatives as Reaction Probes

Donald J. Darensbourg,* Holly Pickner Wiegrefe, and Philip W. Wiegrefe

Contribution from the Department of Chemistry, Texas A&M University, College Station, Texas 77843. Received May 14, 1990

Abstract: Mechanistic aspects of the CO₂ insertion into [Cr(CO)₅H]⁻ to yield [Cr(CO)₅O₂CH]⁻ have been investigated by the examination of the CO₂ exchange reaction: [Cr(CO)₅O₂CH]⁻ + ¹³CO₂ = [Cr(CO)₅O₂¹³CH]⁻ + CO₂. Kinetic measurements show the reaction to be first order in metal substrate concentration and zero order in [¹³CO₂], and the rate is retarded by added [CO]. The activation parameters were determined to be ΔH[‡] = 18.9 ± 0.7 kcal/mol and ΔS[‡] = 12.0 ± 2.9 eu. The value of k_H/k_D was found to be 1.13. The mechanism of this process is dissociative in character, proceeding through the following: (1) CO loss with formation of an intermediate O,O-dihapto species, [Cr(CO)₄(η²-O₂CH)]⁻; (2) rearrangement to an H,O-dihapto chelate (rate-determining step); (3) decarboxylation and recarbonylation; and (4) recarbonylation with ¹³CO₂ in the reverse direction. Consistent with this mechanism, [Cr(CO)₄(η²-O₂CH)]⁻ has been synthesized and identified by IR spectroscopy. To further investigate the decarbonylation step of the mechanism, the energetics of CO loss for a [Cr(CO)₅O₂CR]⁻ derivative were determined from the reaction of [Cr(CO)₅O₂CCH₃]⁻ with P(OCH₃)₃ to afford *cis*-[Cr(CO)₄(P(OCH₃)₃)O₂CCH₃]⁻ + CO. The reaction was found to be first order in metal substrate concentration and to have a small dependence on [P(OCH₃)₃]. The activation parameters for the phosphite-independent pathway were determined to be ΔH[‡] = 18.0 ± 2.2 kcal/mol and ΔS[‡] = -8.8 ± 8.3 eu. These data coupled with the activation parameters for the decarboxylation/recarbonylation reaction afford a well-defined reaction pathway for the C-H bond-forming reaction of CO₂ and [Cr(CO)₅H]⁻. The experimental results are discussed in relation to recent theoretical calculations on the carbon dioxide insertion reaction.

Introduction

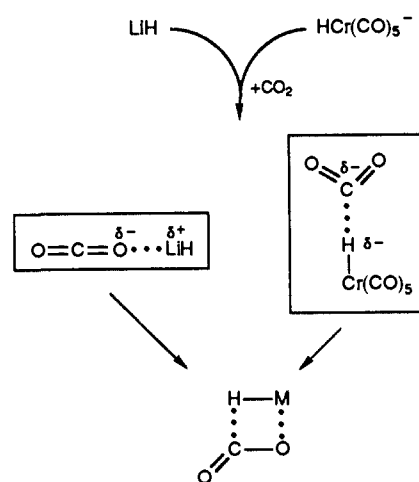
Carboxylation of transition-metal hydrides to afford the 1,2-addition metalloformate product (eq 1) represents an important reaction in the reduction chemistry of carbon dioxide.¹ As indicated in eq 1 the carboxylation reaction is in general reversible. Reaction 1, normally referred to as an insertion of CO₂ into a metal hydride bond, involving the group 6 metal carbonyl hydrides (M = Cr(CO)₅ or W(CO)₅) has been the subject of experimental²⁻⁴ and theoretical studies.⁵ In 1981 when we first reported upon this process, it was described as proceeding via an adduct formed between the very hydridic hydride ligand and the electrophilic carbon center of CO₂.² A similar intermediate was



indeed noted for the analogous interaction of [Cr(CO)₅H]⁻ and BH₃, i.e., [Cr(CO)₅H...BH₃]⁻, which eventually resulted in production of the chelated derivative, [Cr(CO)₄BH₄]⁻.⁶ Because the CO ligands in [Cr(CO)₅H]⁻ were shown not to be labile on the time scale of CO₂ insertion, it was proposed that this adduct formation results in a labilization of the CO ligands with subsequent production of the metalloformate derivative.

Since that initial report a very detailed theoretical study which relies on ab initio calculations has been presented by Bo and Dedieu.⁵ These researchers found that the adduct [Cr(CO)₅-

Scheme I



H...CO₂]⁻ was more stable than its constituents [Cr(CO)₅H]⁻ and CO₂ by 8.4 kcal/mol, and this interaction results in a lowering of the Cr-CO dissociation energy by approximately 7 kcal/mol. A comparable four-membered transition state has resulted from ab initio calculations for the model carboxylation reaction of lithium hydride by Schleyer and co-workers.⁷ Perhaps it is coincidental that the initial interaction of reactants in this instance, which is quite different from that involving [Cr(CO)₅H]⁻ and CO₂, occurring by the way of a linear HLi...O=C=O complex, is also stabilized by 8.4 kcal/mol. Scheme I contrasts the modeling studies for these two carboxylation processes involving alkali and transition-metal hydrides. These processes differ with regard to the extent of ligand lability or unsaturation of the metal and the electropositive character of the metal center.

This presentation is a continuation of our mechanistic investigation on the carbon dioxide insertion reaction of the anionic group 6 metal carbonyl derivatives, in particular enumerating the kinetic parameters of relevance to the process. These complexes represent excellent examples for the study of the carboxylation

(1) (a) Walther, D. *Coord. Chem. Rev.* **1987**, *79*, 135. (b) Behr, A. In *Catalysis in C₁ Chemistry*; Keim, W., Ed.; Reidel: Dordrecht, 1983; p 169. (c) Eisenberg, R.; Hendriksen, D. E. *Adv. Catal.* **1979**, *28*, 79. (d) Darensbourg, D. J.; Kudoroski, R. *Adv. Organomet. Chem.* **1983**, *22*, 129. (e) Ito, T. T.; Yamamoto, A. *Organic and Bioorganic Chemistry of Carbon Dioxide*; Inoue, S.; Yamazaki, N., Eds.; Kodonsha, Ltd.: Tokyo, Japan, 1982; p 79. (f) Palmer, D. A.; van Eldik, R. *Chem. Rev.* **1983**, *83*, 651. (g) Sneed, R. P. A. *Comprehensive Organometallic Chemistry*; Wilkinson, G.; Stone, F. G. A., Abel, E. W., Eds.; Pergamon Press: Oxford, 1982; Vol. 8; p 225. (h) Kolomnikov, I. S.; Grigoryan, M. Kh. *Russ. Chem. Rev.* **1978**, *47*, 334. (i) Braunstein, P.; Matt, D.; Nobel, D. *Chem. Rev.* **1988**, *88*, 747. (j) Behr, A. *Carbon Dioxide Activation by Metal Complexes*; VCH: Weinheim, West Germany, 1988; p 26.

(2) Darensbourg, D. J.; Rokicki, A.; Darensbourg, M. Y. *J. Am. Chem. Soc.* **1981**, *103*, 3223.

(3) Darensbourg, D. J.; Rokicki, A. *Organometallics* **1982**, *1*, 1685.

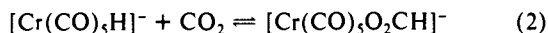
(4) Slater, S.; Lusk, R.; Schumann, B.; Darensbourg, M. Y. *Organometallics* **1982**, *1*, 1662.

(5) Bo, C.; Dedieu, A. *Inorg. Chem.* **1989**, *28*, 304.

(6) Darensbourg, M. Y.; Bau, R.; Marks, M. W.; Burch, R. R., Jr.; Deaton, J. C.; Slater, S. *J. Am. Chem. Soc.* **1982**, *104*, 6961.

(7) Kaufmann, E.; Sieber, S.; Schleyer, P. V. R. *J. Am. Chem. Soc.* **1989**, *111*, 4005.

process because of the detailed information attainable upon observing the behavior of the ancillary carbon monoxide ligands. Hence reaction 2, examined in either direction, should be prototypical of the carboxylation reaction for transition-metal complexes.



Experimental Section

General Methods. All manipulations were carried out in either an argon-filled drybox or on a double-manifold Schlenk vacuum line. Solvents were dried by distillation from the appropriate reagent and degassed prior to use. IR spectra were recorded on an IBM FTIR/32 spectrometer with 0.1 nm NaCl or CaF₂ cells. The photolysis experiments were performed with a mercury-arc 400-W UV immersion lamp, which was purchased from Ace Glass, Inc. ¹H and ¹³C NMR spectra were taken on either a Varian XL-200, XL-200E, or XL-400E superconducting high-resolution spectrometer with an internal deuterium lock, using acetone-*d*₆ (¹H) or THF/acetone-*d*₆ (¹³C) as the solvent. The high-pressure NMR tube was constructed in the department's machine shop according to the specifications of Roe.⁸

Materials. Tetrahydrofuran (THF) was purchased from J. T. Baker Chemical Co. Acetone-*d*₆ was purchased from Cambridge Isotope Laboratories. P(OCH₃)₃ was purchased from Aldrich Chemical Co. and was distilled under nitrogen from sodium benzophenone ketyl before use. Carbon monoxide and CO₂ were purchased from Matheson Gas Products, Inc.; ¹³CO and ¹³CO₂ (99% enriched) were purchased from Isotech, Inc. [PPN][Cr(CO)₅H] (PPN⁺ = bis(triphenylphosphine)iminium cation) was prepared from Cr(CO)₅(piperidine) and [PPN][BH₄] according to the procedure of Slater and Darensbourg.⁹ [PPN][Cr(CO)₅O₂¹³CH] and [PPN][Cr(CO)₅O₂¹³CD] were prepared from reactions of [PPN][Cr(CO)₅H] and [PPN][Cr(CO)₅D] with ¹³CO₂, respectively.^{2,10} [PPN][Cr(CO)₅CCH₃] was synthesized from [PPN][O₂CCH₃] and Cr(CO)₆.¹¹ [PPN][W(CO)₅O₂CH] and [PPN][W(CO)₅O₂CCH₃] were prepared with [PPN][O₂CH] or [PPN][O₂CCH₃] and W(CO)₆, respectively.¹¹ Highly enriched ¹³CO-labeled [PPN][Cr(CO)₅O₂CCH₃] was synthesized by stirring [PPN][Cr(CO)₅O₂CCH₃] under an atmosphere of ¹³CO overnight.¹²

Kinetic Measurements 1. Carbon Dioxide Exchange Reaction of [PPN][Cr(CO)₅O₂CH]. The kinetics of carbon dioxide exchange of [PPN][Cr(CO)₅O₂CH] with ¹³CO₂ to yield [PPN][Cr(CO)₅O₂¹³CH] were monitored by ¹H NMR spectroscopy. In a typical kinetic run, 20 mg of [PPN][Cr(CO)₅O₂CH] was weighed out inside the glovebox. Approximately 1 mL of acetone-*d*₆ was added and the solution was weighed to determine the exact quantity of solvent added. After cooling, by immersing the tube in a dry ice/acetone bath, the atmosphere was evacuated by vacuum and backfilled with ¹³CO₂. On the basis of solubility data determined in THF the solubility of CO₂ at 760 mm of pressure is expected to be greater than 0.3 M. For kinetic measurements below 15 °C the tube was kept in the dry ice/acetone bath until NMR monitoring commenced. The first acquisition was typically started 6–8 min after addition of ¹³CO₂, the time necessary for transfer of the tube into the NMR probe, locking, and shimming. The disappearance of [PPN][Cr(CO)₅O₂CH] was monitored by following the integration of the formate signal (δ 8.28, *d*, *J*_{C-H} = 186 Hz) as a function of time. Data were taken by using an arrayed experiment file with a preset pulse acquisition delay. Integrations were performed with use of a first-order baseline correction program provided by Varian. Pseudo-first-order rate constants and activation parameters were calculated by using least-squares-fitting programs at a 90% confidence limit. The rate constants were determined by a plot of $\ln(I_t - I_i)$ versus time, where *I*_t is the integration of the formate signal at time *t* and *I*_i is integration at infinite time.

2. Carbon Monoxide Substitution of [PPN][Cr(CO)₅O₂CCH₃]. A. The kinetics of CO substitution in [PPN][Cr(CO)₅O₂CCH₃] by P(OCH₃)₃ to yield *cis*-[PPN][Cr(CO)₄(P(OCH₃)₃)O₂CCH₃] and CO were monitored by ¹H NMR. In a typical kinetic determination, 10 mg of [PPN][Cr(CO)₅O₂CCH₃] was loaded into a 5-mm NMR tube. After

the tube was evacuated and backfilled several times with N₂, approximately 1 mL of acetone-*d*₆ was added. The NMR tube was placed into the NMR probe, which was preset to the desired temperature. During the time it took for the solution to reach thermal equilibrium, P(OCH₃)₃ was cooled by immersion in a dry ice/acetone bath. Thirty microliters of P(OCH₃)₃ was added to the solution via syringe, and the tube was inverted to mix reagents. After locking and shimming, the data collection was begun. The reaction progress was followed by measuring the integration of the [PPN][Cr(CO)₅O₂CCH₃] methyl signal (δ 1.61, *s*). Pseudo-first-order rate constants and activation parameters were determined in a manner similar to that described above. **B.** The kinetics of CO loss were also measured by employing carbon monoxide as the incoming ligand. To the ¹³CO-labeled complex, [Cr(¹³CO)₅O₂CCH₃]⁻, was added ¹²CO, and the formation of [Cr(¹³CO)_{5-n}(¹²CO)_nO₂CCH₃]⁻ was followed by ¹³C NMR spectroscopy. In a typical experiment, 40 mg of ¹³CO-labeled [Cr(CO)₅O₂CCH₃]⁻ was loaded in a 10-mm NMR tube. To the solid was added approximately 4 g of acetone-*d*₆, and the solution was cooled by immersion in a dry ice/acetone bath. The nitrogen atmosphere was evacuated by vacuum and an atmosphere of ¹²CO was added. The reaction progress was followed by measuring the disappearance of the *cis*-CO signal (δ 217.7, *m*) as a function of time.

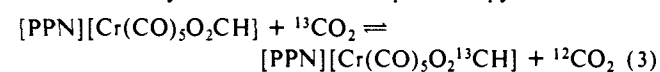
3. Carbon Monoxide Substitution of [PPN][W(CO)₅O₂CH]. The kinetics of CO substitution in [PPN][W(CO)₅O₂CH] by P(OCH₃)₃ to yield *cis*-[PPN][W(CO)₄(P(OCH₃)₃)O₂CH] and CO were monitored by IR spectroscopy. Solution temperatures were controlled by a thermostated water bath, with a precision of ± 0.1 °C. In a typical experiment, to a solution of [PPN][W(CO)₅O₂CH] (90 mg) in THF (6.0 mL) was added 0.23 mL of P(OCH₃)₃ via syringe. Pseudo-first-order conditions were employed with the concentration of phosphite in large (>20-fold) excess over that of the metal complex. Small (0.2 mL) aliquots of the solution were withdrawn periodically and examined by IR spectroscopy. The formation of *cis*-[PPN][W(CO)₄(P(OCH₃)₃)O₂CH] was followed by measuring the absorbance of the $\nu(\text{CO})$ IR band at 2006 cm⁻¹ as a function of time. A base line correction was made on each spectrum by subtracting the absorbance in a region free from reactant, product, or phosphite absorbances. Arbitrarily chosen was the value at 2030 cm⁻¹. Pseudo-first-order rate constants and activation parameters were calculated by using least-squares-fitting programs at a 90% confidence limit. The rate constants were determined by plotting $\ln(A_t - A_i)$ versus time, where *A*_t is the absorbance at infinite time and *A*_i is the absorbance at time *t*. The rate constant for the carbonyl substitution reaction of [PPN][W(CO)₅O₂CCH₃] with P(OCH₃)₃ was measured in a similar manner and previously described.¹³

Determination of *k*_H/*k*_D for the CO₂ Exchange Reaction of [Cr(CO)₅O₂CH]. The kinetics of exchange in [PPN][Cr(CO)₅O₂¹³CH] and [PPN][Cr(CO)₅O₂¹³CD] with ¹²CO₂ to yield [PPN][Cr(CO)₅O₂¹²CH] and [PPN][Cr(CO)₅O₂¹²CD] were monitored simultaneously by ¹³C NMR spectroscopy (400 MHz). A 10-mm NMR tube was charged with an acetone-*d*₆ solution of [Cr(CO)₅O₂¹³CH]⁻ and [Cr(CO)₅O₂¹³CD]⁻ (40 and 60%, respectively, by NMR). The solution was cooled by immersing the tube in a dry ice/acetone bath. The argon atmosphere was evacuated by vacuum and 1 atm of ¹²CO₂ was added. The reaction progress was followed by measuring the disappearance of the [Cr(CO)₅O₂CD]⁻ resonance (δ 168.3, *t*, *J*_{C-D} = 14.4 Hz) and the [Cr(CO)₅O₂CH]⁻ resonance (δ 168.5, *d*, *J*_{C-H} = 94.3 Hz) as a function of time. Spectra were determined with an acquisition time of 1.325 s and a pulse repetition rate of 5 s. The rate constants were determined in a similar manner to those described above.

Synthesis of [PPN][Cr(CO)₄(η^2 -O₂CH)]. The synthesis of this compound was described earlier.¹³ A THF solution of [PPN][Cr(CO)₅O₂CH] (70 mg in 50 mL) was placed in a water-cooled photolysis vessel and a vigorous stream of nitrogen was bubbled through the yellow solution. After the solution was cooled to 5 °C, it was photolyzed for 15 min. The $\nu(\text{CO})$ IR absorbances showed the solution to contain a mixture of [PPN][Cr(CO)₄(η^2 -O₂CH)] ($\nu(\text{CO})$ absorbances at 2002 (*m*), 1871 (*s*), 1852 (*s*), 1813 (*m*) cm⁻¹) and [Cr(CO)₅H]⁻. In solution, the chelated complex decomposed quickly to yield [Cr(CO)₅O₂CH]⁻ and a smaller quantity of [Cr(CO)₅H]⁻.

Results

Carbon Dioxide Exchange Reactions of [PPN][Cr(CO)₅O₂CH]. The CO₂ exchange reaction of [PPN][Cr(CO)₅O₂CH] (eq 3) has been studied by ¹H and ¹³C NMR spectroscopy and shown to



occur quite readily. The ¹³C-enriched product gives rise to a

(8) Roe, D. C. *ACS Symp. Ser.* **1987**, 357, 204. We are sincerely appreciative of the help Dr. C. Roe provided us at several of the stages during the fabrication of this extremely useful device.

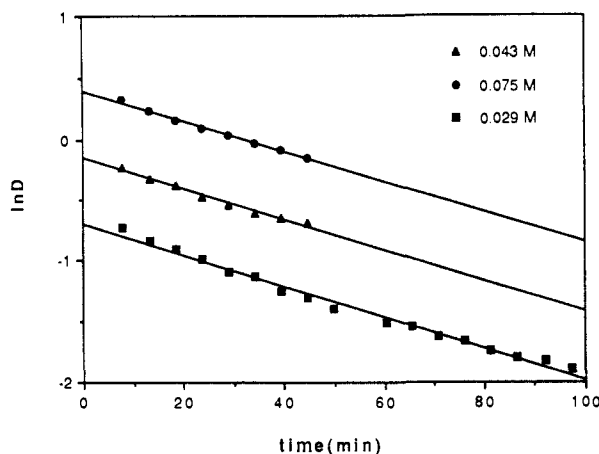
(9) (a) Darensbourg, M. Y.; Slater, S. G. *J. Am. Chem. Soc.* **1981**, 103, 5914. (b) Slater, S. G.; Darensbourg, M. Y. *Inorg. Synth.* **1983**, 22, 181.

(10) Gaus, P. L.; Kao, K. S.; Darensbourg, M. Y.; Arndt, L. W. *J. Am. Chem. Soc.* **1984**, 106, 4752.

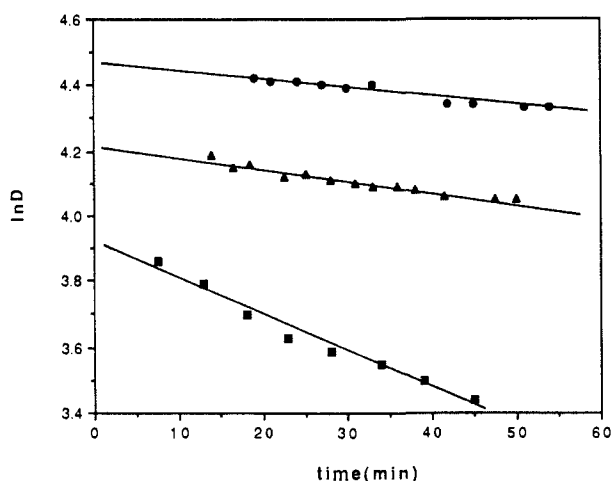
(11) Darensbourg, D. J.; Morse, S.; Ovalles, C.; Pickner, H. C. *Inorg. Synth.* **1990**, 27, 295.

(12) (a) Cotton, F. A.; Darensbourg, D. J.; Kolthammer, B. W. S. *J. Am. Chem. Soc.* **1981**, 103, 398. (b) Cotton, F. A.; Darensbourg, D. J.; Kolthammer, B. W. S.; Kudoroski, R. *Inorg. Chem.* **1982**, 21, 1656.

(13) Darensbourg, D. J.; Wiegrefe, H. P. *Inorg. Chem.* **1990**, 29, 592.



A



B

Figure 1. Kinetic plots of $^{13}\text{CO}_2$ exchange in $[\text{PPN}][\text{Cr}(\text{CO})_5\text{O}_2\text{CH}]$: (A) first-order rate plots as a function of complex concentration; (B) first-order rate plots as a function of added carbon monoxide; (■) no added CO, (▲) 150 psi of CO, (●) 600 psi of CO.

Table I. k_{obs} as a Function of Temperature for the Reaction of $[\text{PPN}][\text{Cr}(\text{CO})_5\text{O}_2\text{CH}]$ with 1 atm of $^{13}\text{CO}_2$

$k_{\text{obs}} \times 10^4, \text{s}^{-1}$	temp, °C	$k_{\text{obs}} \times 10^4, \text{s}^{-1}$	temp, °C
0.12 ± 0.01	0.0	0.49 ± 0.05^b	23.1
0.31 ± 0.01	10.0	0.46 ± 0.06^c	23.1
0.71 ± 0.05	15.0	2.14 ± 0.01	25.0
1.23 ± 0.08	20.0	2.11 ± 0.02	25.0
1.81 ± 0.15^a	23.1	2.08 ± 0.01	25.0

^a 1 atm of $^{13}\text{CO}_2$, carried out in the high-pressure NMR tube. ^b 1 atm of $^{13}\text{CO}_2$ plus 150 psi of CO, carried out in the high-pressure NMR tube. ^c 1 atm of $^{13}\text{CO}_2$ plus 600 psi of CO, carried out in the high-pressure NMR tube.

carbon resonance at δ 168.5 ppm in the formate region, whereas in the proton NMR spectrum the formate singlet at δ 8.28 ppm splits into a doublet with a carbon-hydrogen coupling constant of 186 Hz. This splitting of the formate proton signal upon $^{13}\text{CO}_2$ incorporation was employed in quantifying the rates of the decarboxylation/carboxylation reactions. Typical first-order rate plots as a function of metal complex concentration are provided in Figure 1. The reaction was shown to be first order in the concentration of the metal formate complex and independent of the carbon dioxide pressure when the reaction is carried out in a large excess of $^{13}\text{CO}_2$. That is, in the absence of a sizable contribution from the reverse reaction with $^{12}\text{CO}_2$, reaction 3 is zero order in isotopically labeled carbon dioxide.

Kinetic data determined as a function of temperature are listed in Table I. An Eyring plot of the data contained in Table I

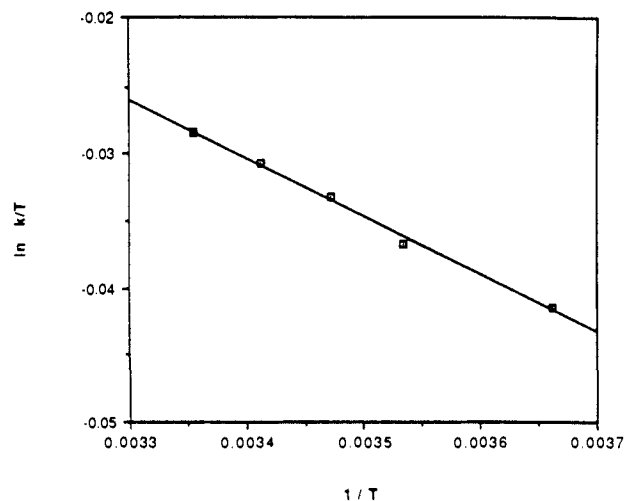


Figure 2. Eyring plot for reaction 3.

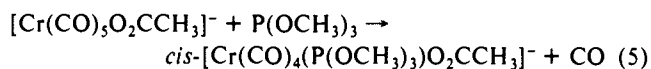
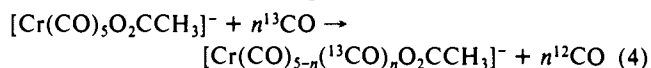
Table II. k_{obs} as a Function of Temperature for the Reaction of $[\text{PPN}][\text{Cr}(\text{CO})_5\text{O}_2\text{CCH}_3]$ with a 20-fold Excess of $\text{P}(\text{OCH}_3)_3$

$k_{\text{obs}} \times 10^4, \text{s}^{-1}$	temp, °C	$k_{\text{obs}} \times 10^4, \text{s}^{-1}$	temp, °C
0.13 ± 0.003	-20.0	1.50 ± 0.02	-10.0
0.16 ± 0.01	-20.0	2.36 ± 0.16	0.0
0.32 ± 0.02	-15.0	5.70 ± 0.92	5.0
1.70 ± 0.08^a	-10.0		

^a Rate determined with a 40-fold excess of $\text{P}(\text{OCH}_3)_3$. This value was not used in the determination of the activation parameters.

(Figure 2) provided activation parameters of $\Delta H^\ddagger = 18.9 \pm 0.7$ kcal/mol and $\Delta S^\ddagger = -12.9 \pm 2.9$ eu. The rate of CO_2 exchange was retarded by added carbon monoxide, with the rate decreasing by a factor of 1.6 upon addition of equal volumes of CO and CO_2 at 1 atm total pressure. Further retardation occurred upon an increase of the CO partial pressure to 150 and 600 psi.

Carbon Monoxide Substitution in $[\text{PPN}][\text{Cr}(\text{CO})_5\text{O}_2\text{CCH}_3]$. The carbon monoxide ligand substitution reactions of $[\text{PPN}][\text{Cr}(\text{CO})_5\text{O}_2\text{CCH}_3]$ with incoming ligands (eqs 4 and 5) have been shown by ^1H and ^{13}C NMR to be facile. Consistent with the *cis*-labilization nature of the acetate ligand, it was demonstrated that CO



was lost stereoselectively in $[\text{Cr}(\text{CO})_5\text{O}_2\text{CCH}_3]^-$.¹² For the reaction of $[\text{Cr}(\text{CO})_5\text{O}_2\text{CCH}_3]^-$ and ^{12}CO , the lability of the *cis*-carbonyl ligands was evidenced by a ^{13}C NMR *cis*-CO signal that decreased as a function of time. The resonance for the *trans*-CO was not affected within the reaction time of 2 h at -20 °C. The substitution rate of the four *cis*-CO ligands was measured, and k_{obs} for the monocarbonyl substitution was calculated. Under an atmosphere of ^{12}CO , k_{obs} for the replacement of one *cis*-CO ligand was determined to be $3.21 \times 10^{-5} \text{ s}^{-1}$ at -20 °C.

For the reaction of $[\text{Cr}(\text{CO})_5\text{O}_2\text{CCH}_3]^-$ and $\text{P}(\text{OCH}_3)_3$, the pseudo-first-order rate constant, k_{obs} , was measured as a function of phosphite concentration. From a range of phosphite concentrations of 0.25 to 0.37 M (20- to 40-fold excess of phosphite concentration over the metal complex concentration), a small dependence of k_{obs} on $[\text{P}(\text{OCH}_3)_3]$ was detected at -10 °C, where the rate constant increased by approximately 6% with a 2-fold increase in $[\text{P}(\text{OCH}_3)_3]$ (see Table II). Hence the reactions were run under pseudo-first-order conditions, with a phosphite concentration approximately 20 times that of the metal complex. Thus in the absence of the small contribution from an I_d process, at $[\text{P}(\text{OCH}_3)_3] \gg [\text{CO}]$, k_{obs} reduces to k_1 (eq 6) *vide infra*. Consistent with this description, for CO ligand substitution re-

$$k_{\text{obs}} = \frac{k_1 k_2 [\text{P}(\text{OCH}_3)_3] + k_{-1} k_{-2} [\text{CO}]}{k_{-1} [\text{CO}] + k_2 [\text{P}(\text{OCH}_3)_3]} \quad (6)$$

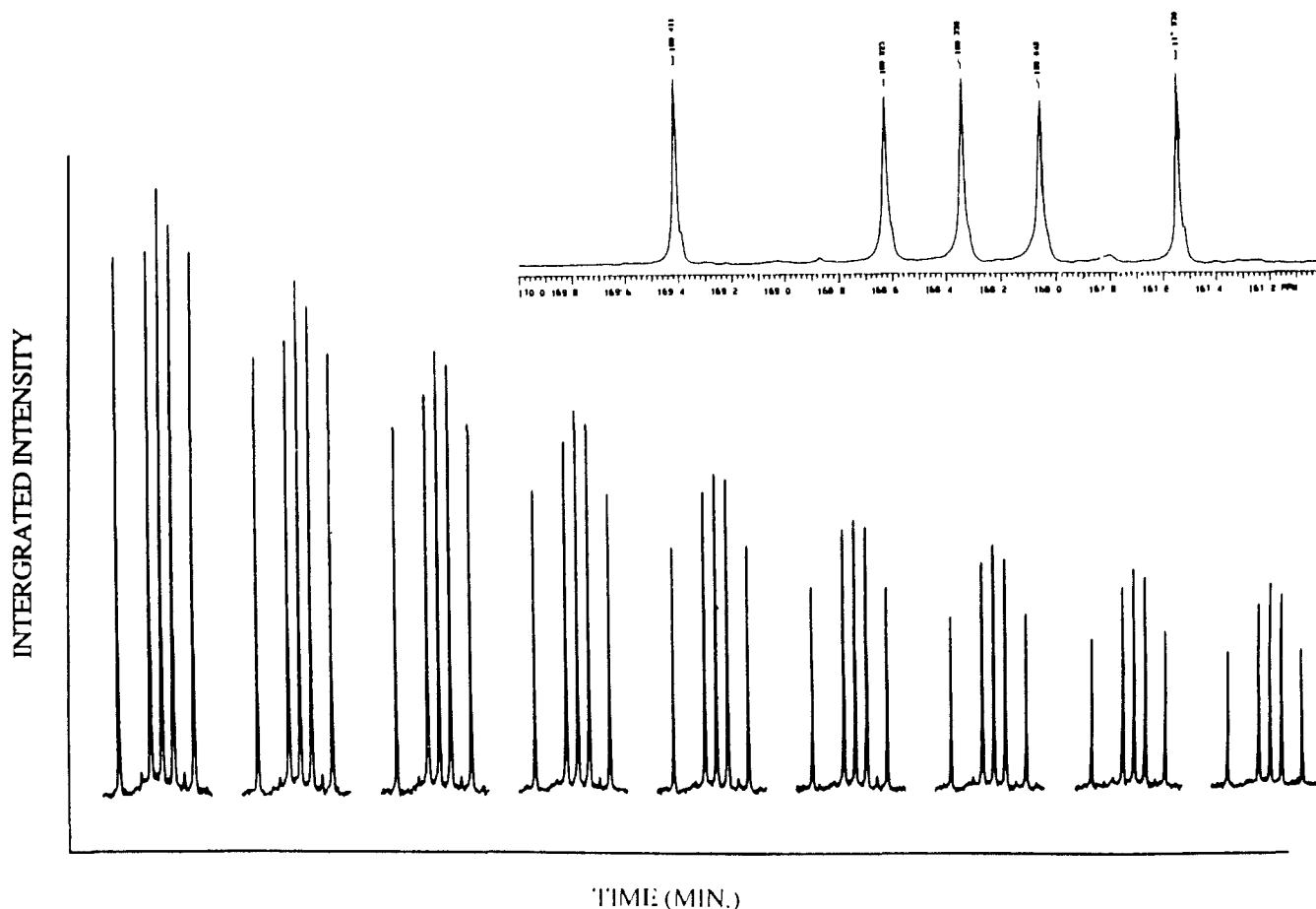
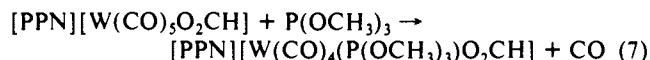


Figure 3. Integrated intensity of the formate ¹H NMR resonance versus time for reactions 8 and 9 at 15 °C, with 32-min intervals between repeating spectral acquisitions. The overlay shows an expanded spectrum of the mixture of [Cr(CO)₅O₂¹³CH]⁻ and [Cr(CO)₅O₂¹³CD]⁻.

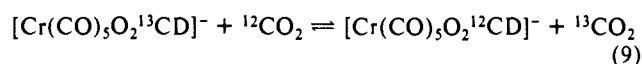
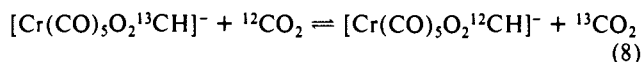
actions of [Cr(CO)₅O₂CCH₃]⁻, $k_{\text{obs}} = 2.4 \pm 0.01 \times 10^{-5} \text{ s}^{-1}$ when P(OCH₃)₃ is the incoming ligand and $k_{\text{obs}} = 3.21 \times 10^{-5} \text{ s}^{-1}$ for the substitution by CO, at -20 °C. Since no significant changes in the reaction rates were observed, we conclude that k_{obs} for both reactions is the CO dissociation rate constant. Kinetic data as a function of temperature are listed in Table II. An Eyring plot of the data in Table II provided the activation parameters, ΔH^* and ΔS^* , $18.0 \pm 2.2 \text{ kcal/mol}$ and $-8.8 \pm 8.3 \text{ eu}$, respectively.

Carbon Monoxide Substitution in [PPN][W(CO)₅O₂CH]. The pseudo-first-order rate constants for CO displacement in the tungsten pentacarbonyl formate species, [W(CO)₅O₂CH]⁻, by P(OCH₃)₃ (eq 7) were determined as a function of temperature



(Table III) via IR spectroscopy. An Eyring plot provided the activation parameters, ΔH^* and ΔS^* , of $22.4 \pm 1.7 \text{ kcal/mol}$ and $1.2 \pm 5.7 \text{ eu}$, respectively. The activation parameters for CO displacement by P(OCH₃)₃ for the acetate derivative, [W(CO)₅O₂CCH₃]⁻, were reported previously as $\Delta H^* = 23.3 \pm 0.8 \text{ kcal/mol}$ and $\Delta S^* = 5.4 \pm 2.6 \text{ eu}$.¹³

Determination of $k_{\text{H}}/k_{\text{D}}$ for the CO₂ Exchange Reaction of [Cr(CO)₅O₂CH]. The kinetic isotope effect was determined for the CO₂ exchange reactions (eqs 8 and 9). The ¹³C NMR spectrum (Figure 3) of the reactant mixture, [Cr(CO)₅O₂¹³CH]⁻



and [Cr(CO)₅O₂¹³CD]⁻, is composed of a doublet and triplet, respectively. To be expected, the triplet is shifted slightly upfield

Table III. k_{obs} as a Function of Temperature for the Reaction of [PPN][Cr(CO)₅O₂CH] with a 20-fold Excess of P(OCH₃)₃

$k_{\text{obs}} \times 10^3, \text{ s}^{-1}$	temp, °C
0.44 ± 0.008	25.0
0.70 ± 0.04	28.9
1.09 ± 0.05	32.0

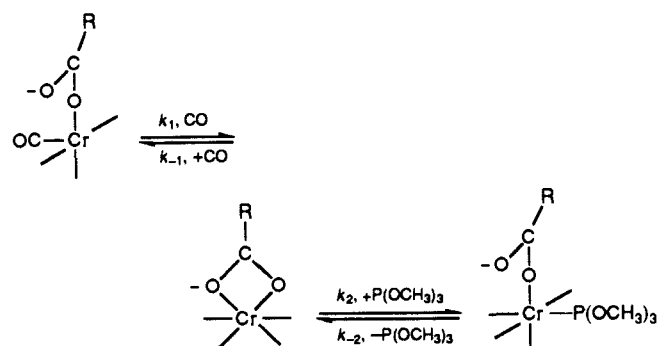
(5 Hz) relative to the doublet centered at δ 168.5 ppm due to the isotopic shift of deuterium. After addition of an atmosphere of ¹²CO₂, the disappearance of both signals was monitored at 15 °C. Pseudo-first-order rate constants for the exchange reaction were determined to be $8.6 \times 10^{-5} \text{ s}^{-1}$ for [Cr(CO)₅O₂¹³CH]⁻ and $7.6 \times 10^{-5} \text{ s}^{-1}$ for [Cr(CO)₅O₂¹³CD]⁻. The calculated value of $k_{\text{H}}/k_{\text{D}}$ is 1.13.

Discussion

As a result of the similarity in the rates of decarboxylation and CO loss in the [Cr(CO)₅O₂¹³CH]⁻ derivative, it was not possible to accurately determine the kinetic parameters for CO displacement in [Cr(CO)₅O₂¹³CH]⁻. Consequently, the kinetic parameters for CO dissociation in the acetate analogue, where decarboxylation does not occur, have been measured. It is nevertheless of importance to establish that changes in the carboxylate ligand from acetate to formate do not have a sizable influence on the rates of CO dissociation. In order to assess this, comparative kinetic studies have been carried out employing the tungsten derivative, since CO loss is much faster than decarboxylation in the [W(CO)₅O₂CH]⁻ species.

As is evident from an examination of the kinetic data listed in Table III for CO dissociation in [W(CO)₅O₂CH]⁻, and previously reported data for the [W(CO)₅O₂CCH₃]⁻ derivative,³ CO dissociation occurs with very similar kinetic parameters in these two cases. For example, the rate constants for CO displacement in [W(CO)₅O₂CH]⁻ and [W(CO)₅O₂CCH₃]⁻ at 25 °C were found

Scheme II



to be $4.40 \pm 0.08 \times 10^{-4}$ and $6.40 \pm 0.10 \times 10^{-4} \text{ s}^{-1}$, respectively, with the activation parameters, ΔH^\ddagger and ΔS^\ddagger , being identical within experimental error. Hence, we feel quite confident that the kinetic data for CO dissociation in the chromium acetate derivative is a good model for the comparable process occurring in $[\text{Cr}(\text{CO})_5\text{O}_2\text{CH}]^-$. It is nevertheless important to note that more dramatic changes in the nature of the carboxylate ligand significantly alter the kinetic parameters for CO displacement in $[\text{W}(\text{CO})_5\text{O}_2\text{CR}]^-$ derivatives.^{14a} Carbon monoxide loss from electron-rich carboxylate metal carbonyls is more facile than CO loss for carboxylates containing electron-withdrawing groups. Concomitantly, it is these electron-rich carboxylates that more readily thermally form oxygen bound η^2 -carboxylate intermediates. That is, as expected the intramolecular ligand-assisted CO dissociation reaction is sensitive to the nucleophilicity of the distal oxygen of the monodentate carboxylate ligand. A detailed investigation of the kinetic parameters for CO displacement in $[\text{W}(\text{CO})_5\text{O}_2\text{CR}]^-$ derivatives as a function of the nature of the R substituent will be presented at a later time.^{14b}

The small value of the enthalpy of activation (18.0 kcal/mol) and the slightly negative entropy of activation (-8.8 eu) for CO loss in $[\text{Cr}(\text{CO})_5\text{O}_2\text{CCH}_3]^-$ are consistent with the intramolecular carboxylate ligand-assisted CO displacement mechanism described previously for the tungsten derivative. However, for the reaction involving the smaller chromium center the associative nature of this process is more pronounced. Indeed if the thermal substitution process is carried out in the absence of incoming ligand, $P(\text{OCH}_3)_3$, infrared spectral evidence for the $[\text{Cr}(\text{CO})_4(\eta^2\text{-O}_2\text{CCH}_3)]^-$ intermediate is observed. Similar infrared spectral evidence for the low-temperature, photochemically generated, formation of the analogous $[\text{Cr}(\text{CO})_4(\eta^2\text{-O}_2\text{CH})]^-$ derivative has been obtained.¹³ Subsequent addition of CO or $P(\text{OCH}_3)_3$ to the chelating carboxylate species led to rapid formation of $[\text{Cr}(\text{CO})_5\text{O}_2\text{CCH}_3]^-$ or *cis*- $[\text{Cr}(\text{CO})_4(\text{P}(\text{OCH}_3)_3)_2\text{O}_2\text{CCH}_3]^-$, respectively (see Scheme II). Although it may be argued that the acetate ligand is acting solely as a *cis* labilizing ligand,¹⁵ with metal distal oxygen interaction occurring after the rate-determining step, this seems less likely in view of the ΔH^\ddagger and ΔS^\ddagger parameters and the dependence on the nature of the R substituent which suggest an associative character to the substitution reaction.

The carboxylate's distal oxygen (O7)-*cis*-carbonyl carbon atom interaction has been modeled with a CHEMX graphic program¹⁶ with use of X-ray structure data.¹² Rotation about the chromium-oxygen bond indicates an average minimum distal oxygen-carbon distance of 2.58 Å. This is illustrated in Figure 4 with use of a space-filling model. In the solid-state structure the plane of the acetate ligand approximately bisects the C(3) and C(4) carbonyl ligands, with the distal oxygen to C(3) and C(4) distances

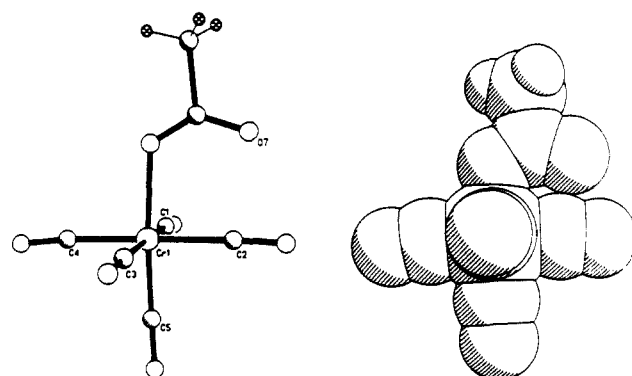
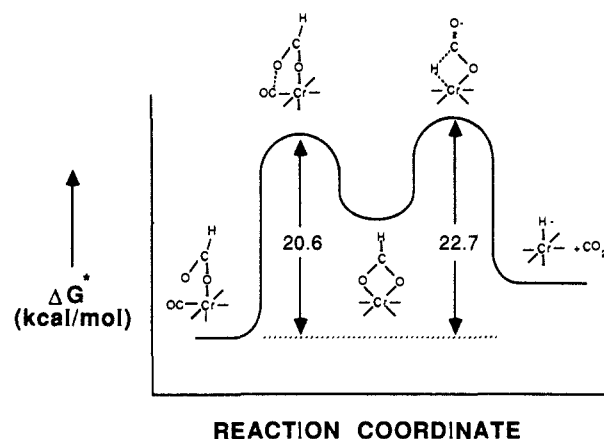


Figure 4. CHEMX model of $[\text{Cr}(\text{CO})_5\text{O}_2\text{CCH}_3]^-$ with bond rotation through the chromium-oxygen bond to minimize the O7 equatorial-C distance, with atom labeling from crystal structure data,¹² as well as the corresponding space-filling model.

Scheme III



being 3.15 and 3.00 Å, respectively.

Assuming CO loss is a requisite step to decarboxylation, ΔG^\ddagger for CO loss must be less than the free energy of activation for the decarboxylation process. This is apparently the case with ΔG^\ddagger for CO loss being 20.6 kcal/mol versus the corresponding value for decarboxylation of 22.7 kcal/mol. Although these activation parameters entail a degree of uncertainty that does not allow for a definitive assessment of their difference, the rate constants clearly differ by an order of magnitude for the two processes with the CO loss process being faster. A schematic representation of the decarboxylation/carboxylation reaction pathway is presented in Scheme III. It should be noted here as well that the calculations of Bo and Dedieu also suggested the η^2 species as possible structures on the insertion pathway.

Since the decarboxylation reaction is not completely quenched under very high pressures of carbon monoxide (see Table I and Figure 1), it is possible that there is an alternative mechanism that does not differ significantly in ΔG^\ddagger from that involving CO loss. That is, at 600 psi of added carbon monoxide, the decarboxylation reaction rate is only slowed down by a factor of 4. Hence although the lowest energy pathway for decarboxylation occurs via CO dissociation, as optional reaction course, possibly a concerted process that does not differ greatly in ΔG^\ddagger , is possible. This would occur by way of a transient structure which resembles that seen in $d^6 \text{ML}_5(\eta^2\text{-H}_2)$ complexes.¹⁷ That is, an interaction like that shown below, made up of an unoccupied metal orbital and the occupied formate fragment (consisting of the π orbitals of CO_2 and the a_1 orbital of the hydride), yields a transition state that does not require an empty coordination site on the metal center.¹⁸

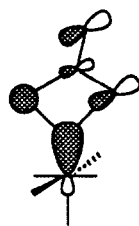
(17) (a) Kubas, G. J. *Acc. Chem. Res.* **1988**, *21*, 120. (b) Crabtree, R. H. *Acc. Chem. Res.* **1990**, *23*, 95.

(18) We are thankful to Dr. A. Dedieu for this suggestion.

(14) (a) For example, the rate of CO loss in $[(\text{CO})_5\text{WO}_2\text{CR}]^-$ derivatives decreases with the electron-withdrawing capability of the R group, with $\text{R} = \text{C}(\text{CH}_3)_3 > \text{CH}_3 > \text{H} > \text{CH}_2\text{CN} > \text{CF}_3$. (b) Darensbourg, D. J.; Joyce, J. *Inorg. Chem.* In press.

(15) For a detailed discussion of *cis* labilization, see: (a) Brown, T. L.; Atwood, J. D. *J. Am. Chem. Soc.* **1976**, *98*, 3160. (b) Lichtenberger, D. L.; Brown, T. L. *J. Am. Chem. Soc.* **1978**, *100*, 366.

(16) CHEMX, developed and distributed by Chemical Design Ltd., Oxford, England.



The small kinetic isotope effect ($k_H/k_D = 1.13$) observed for the decarboxylation reaction is indicative of an early transition state for hydrogen transfer from the carbon atom of the formate ligand to the metal center. This observation is consistent with Bo and Dedieu's calculations⁵ which reveal significant C-H interaction in the adduct formed prior to the CO₂ insertion process.

For example, the C-H distance in the proposed adduct $[\text{Cr}(\text{C}-\text{O})_3\text{H}\cdots\text{CO}_2]^-$ of 1.15 Å is quite close to the anticipated value in the formate ligand.¹⁹ On the other hand in instances involving a less hydridic hydride ligand where adduct formation should be less significant, a larger kinetic isotope effect would be expected. This is indeed observed in the kinetic isotope effect ($k_H/k_D = 1.55$) for the decarboxylation of $\eta^5\text{-C}_5\text{H}_5\text{Re}(\text{O}_2\text{CH})(\text{NO})\text{PPh}_3$.²⁰

Acknowledgment. The financial support of this research by the National Science Foundation (Grant CHE 88-17873) and the Robert A. Welch Foundation is greatly appreciated.

(19) Darensbourg, D. J.; Day, C. S.; Fischer, M. B. *Inorg. Chem.* **1981**, 20, 3577.

(20) Merrifield, J. H.; Gladysz, J. A. *Organometallics* **1983**, 2, 782.

Single-Crystal, Solid-State, and Solution ¹¹³Cd NMR Studies of $[\text{Cd}(\text{SR})_2(\text{N-donor})_2]$ Complexes. Structural and Spectroscopic Analogues for Biologically Occurring $[\text{M}(\text{S-Cys})_2(\text{His})_2]$ Centers

Rodolfo A. Santos, Eric S. Gruff, Stephen A. Koch,* and Gerard S. Harbison*

Contribution from the Department of Chemistry, State University of New York at Stony Brook, Stony Brook, New York 11794-3400. Received March 13, 1990

Abstract: A series of compounds of the formula $[\text{Cd}(\text{SR})_2(\text{N-donor})_2]$ has been synthesized, characterized by X-ray crystallography, and studied by solid-state and solution ¹¹³Cd NMR spectroscopy to serve as analogues for biologically occurring $[\text{M}(\text{S-Cys})_2(\text{His})_2]$ centers. The compounds include $[\text{Cd}(\text{S-2,4,6-}i\text{-Pr}_3\text{-C}_6\text{H}_2)_2(\text{bpy})]$ (1), $[\text{Cd}(\text{S-2,4,6-}i\text{-Pr}_3\text{-C}_6\text{H}_2)_2(\text{phen})_2]$ (2), $[\text{Cd}(\text{S-2,4,6-}i\text{-Pr}_3\text{-C}_6\text{H}_2)_2(1\text{-Me-imid})_2]$ (3), and $[\text{Cd}(\text{S-2,4,6-}i\text{-Pr}_3\text{-C}_6\text{H}_2)_2(1,2\text{-Me}_2\text{-imid})_2]$ (4). Compounds 1-3 have been characterized by X-ray crystallography. The unit cell parameters are as follows. For 1: $a = 15.081$ (9) Å, $b = 14.716$ (9) Å, $c = 17.72$ (1) Å, $\beta = 100.36$ (5)°, $V = 3868$ (8) Å³, $Z = 4$, $P2_1/c$. For 2: $a = 10.12$ (2) Å, $b = 16.56$ (1) Å, $c = 23.50$ (2) Å, $\beta = 92.1$ (5)°, $V = 3934$ (14) Å³, $Z = 2$, $P2_1/n$. For 3: $a = 16.541$ (7) Å, $b = 15.887$ (6) Å, $c = 16.36$ (1) Å, $\beta = 108.91$ (5)°, $V = 4068$ (7) Å³, $Z = 4$, $P2_1/c$. Compounds 1-4 have been characterized by solution and CP/MAS ¹¹³Cd spectroscopy. The ¹¹³Cd shielding tensors of 1 have been obtained from a single-crystal study ($\sigma_{11} = 814$ ppm, $\sigma_{22} = 630$ ppm, $\sigma_{33} = 32$ ppm). Similar large chemical shielding anisotropies (CSA) were also observed for 2-4. The solution ¹¹³Cd NMR spectra are consistent with monomeric $[\text{Cd}(\text{SR})_2(\text{N})_2]$ structures. The large difference in the ¹¹³Cd chemical shift for 2 in the solution and solid state is explained by the weak dimeric structure of 2 in the solid state. The implications of the large CSA to solution and solid-state measurements of related centers in proteins are discussed.

Recently, a wide variety of metalloproteins containing or believed to contain a $[\text{Zn}(\text{S-Cys})_2(\text{His})_2]$ site have been discovered.¹ Prominent in this group are a major class of the "zinc finger" proteins, which include transcription factor IIIA (TFIIIA)^{1,2} and, most recently, in the human immunodeficiency virus type I enhancer binding protein (HIV-EPI).³ This coordination center had previously been observed in the imidazole-inhibited active site of liver alcohol dehydrogenase (LADH).⁴ Since zinc is a spectroscopically silent metal, cadmium and cobalt complexes have been substituted in the native proteins to further aid in the study of the spectroscopic features of zinc centers.⁵ We have been synthesizing and studying the properties of a series of potential models, $[\text{M}(\text{SR})_2(\text{N-donor})_{(4-x)}]$ ($\text{M} = \text{Zn}, \text{Co}, \text{Cd}$) for cyste-

ine-containing zinc metalloproteins.⁶

Cadmium is often substituted in the proteins and used to aid in the determination of the coordination environment of the native metal, primarily because of the usefulness of ¹¹³Cd NMR.^{7,8} The chemical shift range of ¹¹³Cd NMR exceeds 900 ppm and the technique is widely regarded as one of the most useful methods for aiding in the determination of the coordination sphere of a wide range of cadmium compounds. It has been shown that the trends in proteins for chemical shift vs ligand type follow those seen for simple coordination complexes [i.e., thiolate ligands are most strongly deshielding, while nitrogen and oxygen donor ligands have a weaker deshielding effect on the Cd(II) ion], but the effect of coordination number, geometric distortions, and ligand charge

(1) (a) Klug, A.; Rhodes, D. *Trends Biochem. Sci.* **1987**, 12, 464. (b) Evans, R. M.; Hollenberg, S. M. *Cell* **1988**, 52, 1. (c) Berg, J. M. *Prog. Inorg. Chem.* **1989**, 37, 143.

(2) Miller, J.; McLachlan, A. D.; Klug, A. *EMBO J.* **1985**, 4, 1609.

(3) van Wijnen, A. J.; Wright, K. L.; Lian, J. B.; Stein, J. L.; Stein, G. S. *J. Biol. Chem.* **1989**, 264, 15034.

(4) Ekland, H.; Samama, J.-P.; Wallén, L. *Biochemistry* **1982**, 21, 4858.

(5) Vallec, B. L. In *Zinc Proteins*; Spiro, T. G., Ed.; Wiley-Interscience: New York, 1983.

(6) (a) Corwin, D. T., Jr.; Fikar, R.; Koch, S. A. *Inorg. Chem.* **1987**, 26, 3079. (b) Corwin, D. T., Jr.; Gruff, E. S.; Koch, S. A. *J. Chem. Soc., Chem. Commun.* **1987**, 966. (c) Corwin, D. T., Jr.; Gruff, E. S.; Koch, S. A. *Inorg. Chim. Acta* **1988**, 151, 5. (d) Corwin, D. T., Jr.; Koch, S. A. *Inorg. Chem.* **1988**, 27, 493. (e) Gruff, E. S.; Koch, S. A. *J. Am. Chem. Soc.* **1989**, 111, 8762.

(7) Summers, M. F. *Coord. Chem. Rev.* **1988**, 86, 43.

(8) Otvos, J. D.; Armitage, I. M. In *Biochemical Structure Determination by NMR*; Marcel Dekker: New York, 1982.